

Numerical Analysis of Natural Convection Effects in Latent Heat Storage Using Different Fin Shapes

Lippong Tan, Yuenting Kwok, Ahbijit Date, Aliakbar Akbarzadeh
 School of Aerospace, Mechanical, Manufacturing Engineering, RMIT University
 Melbourne, Australia
 lippong.tan@rmit.edu.au

Abstract-A numerical investigation was carried out to evaluate the melting characteristics of phase change material (PCM) in an inner fin type rectangular encapsulation using different fin shape configurations. Despite straight fins are the commonly used in PCM thermal storage for heat transfer enhancement mechanism, increasing the number of fins can significantly hamper the natural convection effects which will only lead to a marginal improvement in heat transfer rate. Hence, exploring different geometrical fin shapes can be another option to improve heat transfer rate or served as an alternative method for thermal enhancement in latent heat storage system. This paper presents extensive computational simulation on the PCM melting in four different investigated fin shapes: straight fin, T-shape fin, Y-shape fin and cross-shape fin configurations. Fluent 6.3 simulation software was utilized in producing two-dimensional simulation to visualize the PCM melting fractions, temperature distributions and flow fields of the melting process internally. The results had shown that changing the geometrical fin shape was able to deliver comparable melting performance as the conventional straight fin configuration. The natural convection current formations and circulation patterns will be discussed in this paper.

Keywords-PCM; melting; fin shape; convection current; CFD

I. INTRODUCTION

Latent heat storage system plays important roles in energy conservation for environmental and civil engineering. Solar heating system is one of the examples used in civil engineering where phase change materials (PCM) are utilized for storing thermal energy dissipated by the sun during day and reuse the stored heat for heating water supply in buildings.

Latent heat storage has higher heat storage density than sensible heat storage due to the present of latent heat of fusion in which material undergoes phase change. For instance, a typical rock-based sensible heat storage requires seven times of storage mass compared to paraffin 116 wax for storing the same amount of heat energy [1-2]. Latent heat storage system undergoes isothermal operation upon reaching the PCM melting range and the required operating temperature and duration can be sized through selection of the respective PCM thermo-physical properties. Because of this high heat capacity capability, this technology is further exploited in electronic cooling where it is used for thermal management of the electronic devices [3].

In spite of having high energy storage density and isothermal operation offered by latent heat storage, sensible heat storage is still the preferred method for thermal storage

system design. This is due to the poor thermal conductivity of the PCM which limits the rate of heat absorbing and releasing during melting and freezing respectively. Organic PCM such as paraffin wax delivered acceptably high heat storage density (~ 200 kJ/kg) with wide range of melting temperatures. They are chemically stable, high thermal cyclic and no phase segregation which make them ideal PCM for the thermal storage system. However, the low thermal conductivity (~ 0.2 W/m K) has greatly limited their potentials and applications. Despite inorganic PCM (salt hydrate) has higher thermal conductivity (~ 0.5 W/m K) and greater energy density (~ 450 KJ/kg), phase segregation and supercooling are serious issue posed in thermal storage design. To embark on economical and feasible storage system, using simple but effective ways for improving the poor thermal conductivity of organic PCM will be the prospective direction for future latent heat storage development. Without having a cost effective solution on PCM thermal enhancement, this technology will still remain as unsuccessful for large scale applications. Published literatures [4-5] have reviewed on various thermal enhancement methods for improving the heat transfer performance of latent heat storage systems. These approaches are: using extended surface (fins), employing multiple PCM's method, metal matrix, metallic fillers and micro-encapsulation. In this present investigation, using extended surface (fins) as thermal enhancement method will be explored and discussed.

Using high thermal conductive fins in thermal storage is one of the simple and effective approaches for improving the melting rate of PCM in the thermal storage. However, increasing the number of metallic fins will only improve the effective thermal conductivity of the system and will not lead to a sharp improvement of the overall heat transfer coefficient. This is because natural convection heat transfer effect is diminished within the smaller fin gap volume. Gharebagi and Sezai [6] had investigated the performance of rectangular PCM device with horizontal fins added to heated vertical walls. They found out that with the increasing of fins only lead to a marginal increase in heat transfer rate. Thus, they concluded that increasing number of fins would hamper the effect of natural convection within the system and melting become a conduction-dominated process. It is noted that during melting, only conduction heat transfer is possible in solid state and natural convection become dominance when in liquid state or during phase transition. Lacroix and Benmadda [7] did numerical studies on a rectangular enclosure with horizontal fins extending into the PCM from heated wall. It was concluded that a few longer fins were more effective in increasing the melting rate than using a large number of shorter

fins. The larger gap size within the fins unrestricted the growth of natural convection effects in the enclosure.

The authors noted that heat transfer dominancy varies from solid to liquid state during melting. Improving the effective thermal conductivity in solid will be ideal as heat is transferred to the solid PCM by conduction at initial stage of melting. As melting continues, thermal resistance in the liquid region will increase as growing volume of liquid PCM are formed near the heating walls and fins. This is due to the liquid PCM normally has lower thermal conductivity ($\sim 0.15\text{W/m K}$) than in solid state ($\sim 0.2\text{W/m K}$), heat transfer by conduction will gradually decline with the thickening of the liquid zone and reduce the overall heat transfer coefficients. Hence, improving the natural convection heat transfer effects which driven by the temperature gradient within the liquid zone will be a better approach for thermal enhancement. Lamberg et al. [8] had proven the natural convective effect by conducting an experimental and numerical study on melting performance of PCM in a rectangular enclosure, with and without natural convection effect. The results showed that PCM took double the time to reach the maximum temperature when natural convection effect was ignored. Jellouli et al. [8] also did a similar experiment on melting of PCM in rectangular enclosure but with heating at the bottom. The isotherms obtained were horizontal at the early stage and became accentuated at the latter stage. Based on this phenomenon, he concluded that conduction dominated melting process at the early stage and gradually shifted to natural convection effect during melting test.

The aim of this work is to investigate numerically on the melting behaviors and performance of using different inner fin shapes in a rectangular encapsulation. Based on the literature, increasing number of convectional straight fins does not improve the melting rate linearly. The authors investigate the alternative way by exploring the PCM melting effect of using different fin shape configurations by incorporating and relocating of horizontal fins to vertical straight fins. These proposed fin shapes in this investigation are T-shape, Y-shape and cross-shape where its geometrical fin shapes will influence the conduction and natural convection heat transfer during melting process.

II. NUMERICAL ANALYSIS

In this section, four different rectangular encapsulations with different inner fin shapes were numerically investigated. Commercial CFD simulation software (Fluent 6.3) was used to solve the conservation equations for mass, momentum and energy. The physical model and the computational procedure are presented in detail in this section.

A. Physical Model

Schematic two-dimensional computational domains for four different cases were illustrated in figure 1. To perform a comparative melting performance analysis, all the fin configurations were sized to their respective perimeter to achieve common PCM volume. Originally, the rectangular thermal storage was designed with four inner aluminum fins. Due to symmetry of the rectangular geometry, only half of the

encapsulation would be used in the modeling for time and memory saving during computational process.

The computation properties of PCM and aluminum are listed in table 1.

TABLE I. MATERIALS PROPERTIES IN SIMULATION

Parameters	Aluminum	PCM
Thermal conductivity (W/m K)	202.4	0.2
Density (kg/m ³)	2719	$880[1 - 0.001(T - 320)]$
Specific heat (J/kg K)	871	2500
Latent heat (kJ/kg)	-	140
Melting temperature (°C)	-	43-49

The reason for using T-shape fin, Y-shape fin and cross-shape fin is to investigate the influence of melting effect in different fin shape configurations. The intention for using these distinctive T-shape and cross-shape and Y-shape fins was to observe the natural convection currents (vortices) formed during melting. In order to have similar fin heights for all configurations, the number of fins for the straight fin type will be doubled. Constant heat flux of 1000W/m² was supplied to the base of the encapsulation.

Boussinesq approximation was adopted to calculate the change in PCM density as a function of temperature in the liquid density given by:

$$\rho = \rho_o [1 - \beta(T - T_m)] \quad (1)$$

And the relationship of buoyancy forces in the momentum equation is given by:

$$-\rho g = \rho_o g [\beta(T - T_m) - 1] \quad (2)$$

where ρ_o is the reference density at melting temperature T_m and β is the thermal expansion which valued at 0.001 based on the data provided by Humphries and Griggs [9]. The dynamic viscosity of the liquid PCM is given by [10]:

$$\mu = 0.001 \times \exp\left(-4.25 + \frac{1790}{T}\right) \quad (3)$$

B. Governing Equations

Enthalpy-porosity formulation [7] was adopted in solving phase change region in PCM. Similar set of governing equations used in the computation were referenced from Shatikan et al. [11] where he simulated the PCM melting in rectangular fin-type partition storage. In this numerical study, volume of fluids (VOF) which used for simulating the two or more different fluids is not considered and volumetric expansion of PCM is negligible in this computational analysis.

Continuity:

$$\frac{\partial}{\partial x_i} (\rho u_i) = 0 \quad (4)$$

Momentum:

$$\frac{\partial}{\partial t} (\rho u_i) + \frac{\partial}{\partial x_i} (\rho u_i u_j) = \mu \frac{\partial^2 u_i}{\partial x_i \partial x_j} - \frac{\partial P}{\partial x_i} + \rho g_i + S_i \quad (5)$$

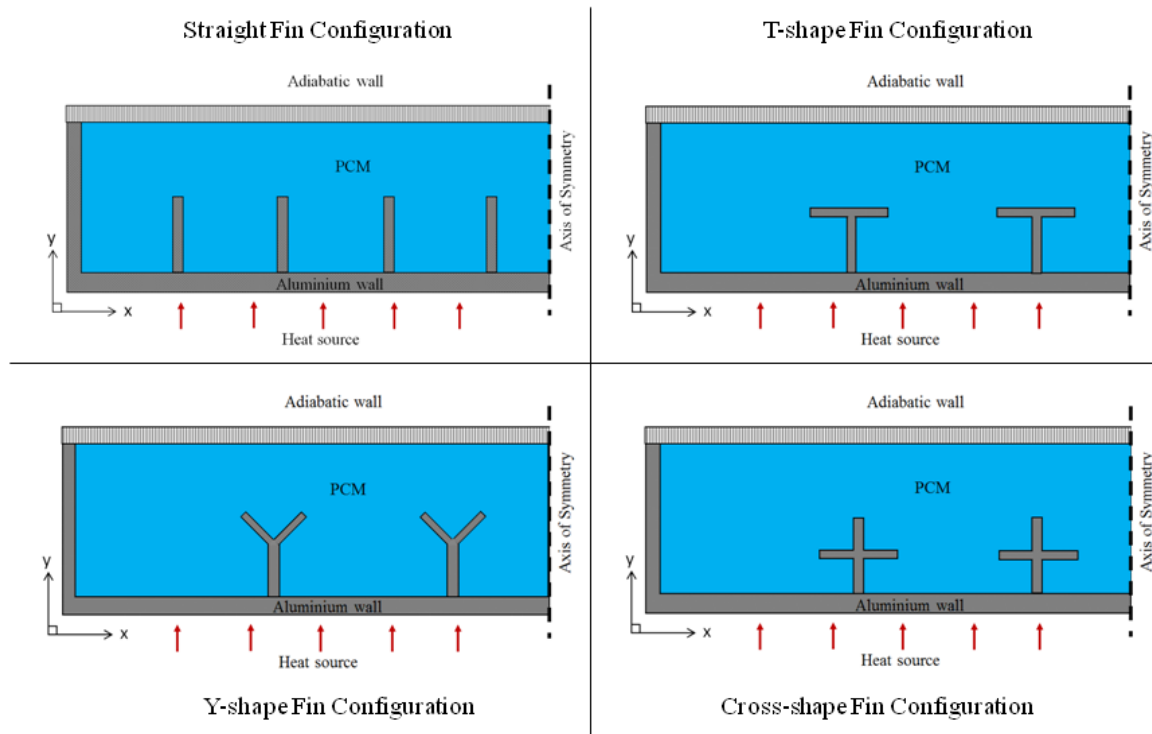


Figure 1 Computational domains for straight fin (8 fins), T-shape (4 fins), Y-shape (4 fins) and Cross-shape (4 fins) configurations

Energy:

$$\frac{\partial}{\partial t}(\rho h) + \frac{\partial}{\partial x_i}(\rho u_i h) = \frac{\partial}{\partial x_i} \left(k \frac{\partial T}{\partial x_i} \right) \quad (6)$$

Where ρ is the density, k is the thermal conductivity, μ is the dynamic viscosity, S_i is the momentum source term, u_i is the velocity component, x_i is the Cartesian coordinate and h is the specific enthalpy. The sensible enthalpy h_s is given by:

$$h_s = h_{ref} + \int_{T_{ref}}^T C_p dT \quad (7)$$

And the total enthalpy, H is defined as:

$$H = h_s + \Delta H \quad (8)$$

The total enthalpy is the sum of sensible enthalpy h_s and the enthalpy change due to phase change γL , where h_{ref} is the reference enthalpy at the reference temperature T_{ref} , C_p is the specific heat, L is the specific enthalpy of melting (liquid state) and γ is the liquid fraction during the phase change which occur over a range of temperatures $T_s < T < T_l$ defined by the following relations:

$$\gamma = \frac{\Delta H}{L} = 0 \quad \text{if} \quad T_s < T \quad [\text{Solid}] \quad (9)$$

$$\gamma = \frac{\Delta H}{L} = \frac{T - T_s}{T_l - T_s} \quad \text{if} \quad T_s < T < T_l \quad [\text{Mushy}] \quad (10)$$

$$\gamma = \frac{\Delta H}{L} = 1 \quad \text{if} \quad T > T_l \quad [\text{Liquid}] \quad (11)$$

The source term S_i in the momentum equation (eqn. 5) is given by:

$$S_i = -A(\gamma) u_i = \frac{C(1-\gamma)^2}{\gamma^3 + \epsilon} u_i \quad (12)$$

Where $A(\gamma)$ is defined as the “porosity function” which governed the momentum equation mimic Carman-Kozeny equations for flow in porous media introduced by Brent et al. [12]. The function reduces the velocities gradually from a finite value as 1 in fully liquid to 0 in fully solid state within the computational cells involving phase change. The epsilon $\epsilon=0.001$ infinity avoidance constant due to division by zero and C is a constant reflecting the morphology of the melting front where $C = 105$ was assumed in this study which had been used in by Shatikan et al. [11].

C. Computational Procedure

The SIMPLE algorithm has been used for solving the mass, momentum and energy governing equations. Approximately about 150,000 triangular and quadrilateral cells were meshed for all configurations for solving the flow fields, melt fractions

and temperature distributions. The time step selected was 0.1 second where comparative testing on time step of 0.01, 0.05 and 0.1 seconds had shown little difference which deemed to be neglected. Hence, larger time step of 0.1 second can be used for saving computational time. The maximum number of iteration for every time step was between 10 and 20 as recommended by Fluent [13].

III. RESULTS AND DISCUSSIONS

In this section, simulation for PCM melting were developed and discussed. As the experimental prototypes were made of aluminum, melting process is not visible during testing. The developed computational visualizations will be used as a predictive tool for melting observation

A. Experimental Setup for Validation

The experimental prototypes for the investigating fin shape configurations were still in the stage of fabrication and model validation on actual prototypes was not possible. However, an independent experiment was conducted on existing rectangular PCM encapsulation showed in figure 2 has similar physical dimensions except for geometry of the installed fins. The achieved experimental data would be used for validating the computational method as it would be similarly modelled.



Figure 2 Experimental prototype (4 straight fins slab)

The physical dimensions of the PCM slab are 300mm (length) x 300mm (width) x 25mm (depth). A total of nine T-type thermocouples were located at different locations shown in figure 3 for recording temperatures during phase change process.

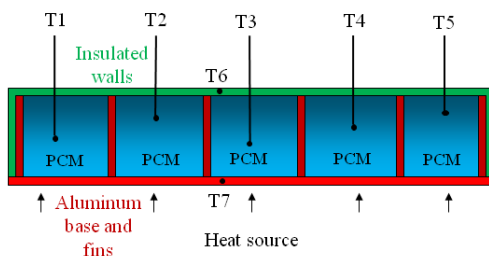


Figure 3 Schematic diagram for fin-type PCM slab and thermocouple locations.

Thermocouples 1-5 showed in figure 3 were used for measuring the PCM temperature at different heights during melting. Thermocouple 6 and 7 were used to capture the top (Perspex sheet, 3mm thick) for accounting heat loss and the bottom of aluminum plate. All exposed surface of the slab was

fully insulated using glass wools which had a high thermal resistance of $\sim 280\text{C/W}$. The heater used was hot plate stirrer (model 209-1) from IEC Pty Ltd and the data acquisition unit used was Agilent 34970A for capturing the respective temperature at timely basis. The PCM used in the experimental validation and numerical investigation was paraffin wax. The summarized thermo-physical properties are detailed in table 2.

TABLE II. THERMOPHYSICAL PROPERTIES OF PARAFFIN WAX

Parameters	Values
Density [kg/m^3]	880 (solid)/760 (liquid)
Specific heat [kJ/kg K]	2.9 (solid)/2.2 (liquid)
Thermal conductivity [W/m K]	0.2
Melting temperature [$^{\circ}\text{C}$]	47
Latent heat [kJ/kg]	140
Thermal expansion [K^{-1}]	0.001

B. Model Validation

Model validation was performed by comparing of the numerically predicted temperature data with experimental data showed in figure 4.

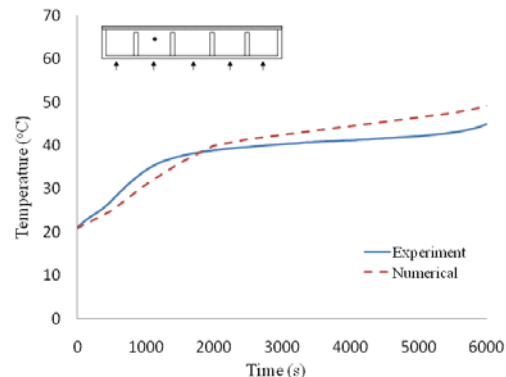


Figure 4 Experimental and numerical temperature distributions comparison

The numerical and experimental temperature history at the thermocouple location (T2) was compared. The validation showed good agreement between both data over experimental time where both results stayed within 40°C .

C. Melting Fraction Performance

Melt fraction representation evaluates the melting performance of PCM in different heat enhancement configurations with respect to time. Figure 5 shows the simulated melting patterns in the same rectangular encapsulation but with different geometrical fin shapes installed internally. Three different stages of melting: 1000 seconds, 2000 seconds and 4000 seconds were visually captured for the melt fraction, temperature distributions and flow fields analysis. Based on the simulation, all fin shape configurations have shown similar melting patterns at early stage of melting (1000 seconds) where the melt fronts were formed at the aluminum walls and fins surfaces. This was due to higher thermal conductivity ($\sim 200\text{W/m K}$) of the aluminum material which allow higher heat conduction rate to the surrounding PCM. However, the melting phenomenon became very different when the liquid fraction of the melted PCM

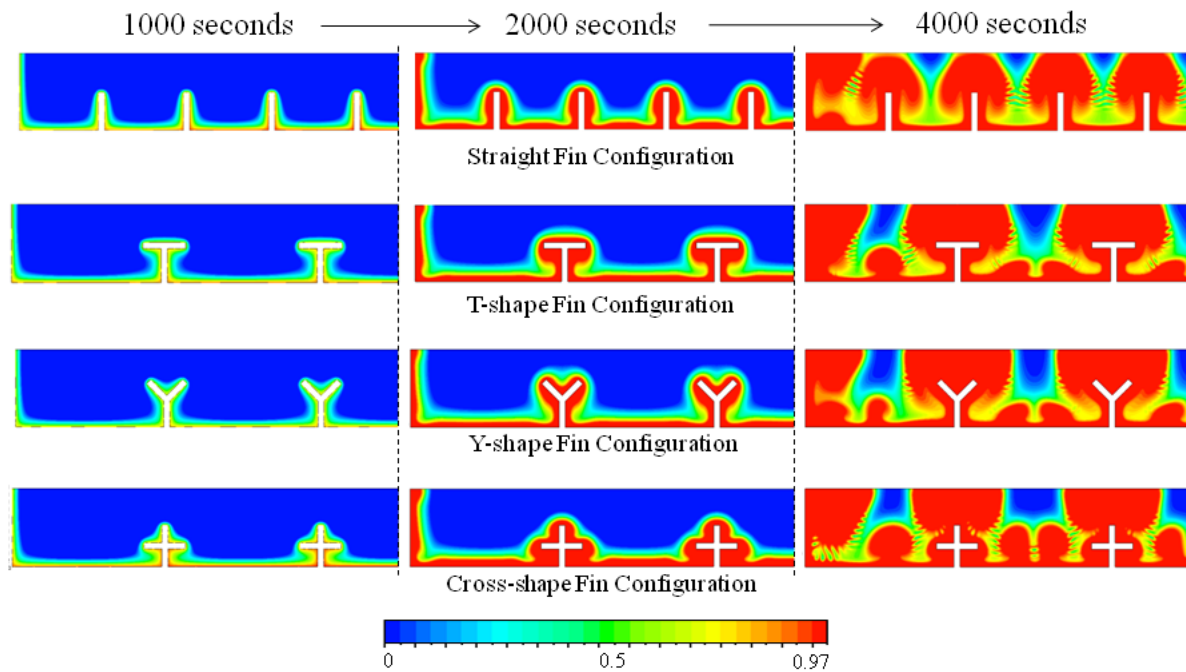


Figure 5 Melt fraction visualization of straight fin, T-shape fin, Y-shape fin and Cross-shape fin type at 1000s, 2000s and 4000s of melting.

became greater at the later stages (2000 seconds and 4000 seconds). As mentioned earlier, the natural convection effect would become dominance with the growing liquid formation in the rectangular encapsulation. The density of the PCM has a decreasing function as the temperature rises which cause the buoyancy effect. Hence, natural convection currents (vortices) were driven by temperature gradients within the liquid zone.

At 2000 seconds time stage, the greater difference in melting was seen in all the four configurations. The cross-shape fin and T-shape fin had wider melt front at bottom and middle region respectively. Both melting patterns have thicker liquid fraction as compared to straight fin especially at the horizontal side fins regions where it extended into the core of the PCM. The present of horizontal fins improved melting by allowing more small multiples vortices formation at different elevated region which will be discussed in the later section. The side fins for Y-shape fin configuration was angled at 45° to the top surface did not have similar melting pattern as T-shape fin and cross-shape fin configurations. Side fin orientation does have some impact on melting behavior and natural convective vortices formation. As heating continued, the melting patterns in stage 4 were totally different than in stage 2. It is important to note that PCM melting pattern will be irregular due to the present of natural convection effect in which vortices driven by temperature difference.

Figure 6 shows the melt fraction comparison of the four investigated fin shapes. Based on the numerical results, the difference in liquid formation among all configurations are very small. However, it has demonstrated that by changing the geometrical fin shapes are able to deliver the similar melting performance of using more conventional straight fins (double in fin number). In precise analysis, cross-shape fin has better melting performance at the first half of the melting process and degraded at the latter stage. Both T-shape and Y-shape fins

have similar performance where both configurations perform well in the middle of the process. Straight fins configuration has poorer melting performance at the earlier stage despite having more fins installed. However, its melt performance is the best at the later stage when the liquid fraction becomes greater.

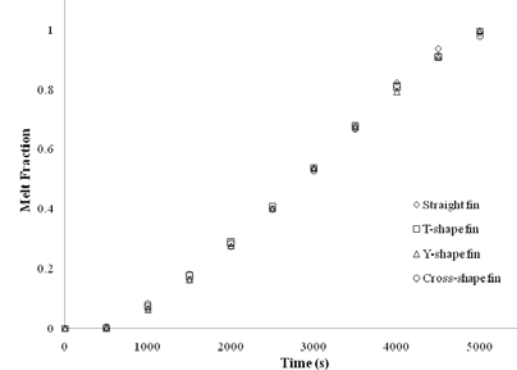


Figure 6 Melt fraction comparison: Straight fins, T-shape fins, Y-shape fins and Cross-shape fins.

D. Natural Convective Effects and Temperature Distributions

Figure 7 shows the temperature distributions and natural convective flow fields at 2000 seconds of constant heating. Thicker melt fronts were seen forming around the T-shape, Y-shape and cross-shape than straight fin configuration. This phenomenon is due to the present of multiple regions of small natural convective vortices circulating around aluminum surfaces. T-shape and Y-shape fins have lower temperature gradient internally due to the present of side fins in the middle section of the rectangular encapsulation. These side fins will assist in generating more solid-liquid interfaces into the core of

PCM and promote greater natural convective heat transfer within the liquid zones. Wider radius of convective vortices circulation was seen at these fin regions compared to the straight fin configuration. However, cross-shape fin configuration has an adverse effect where its side fins were positioned closer to the bottom of the heating base and developed high temperature region. The close gap which enclosed by higher thermal conductivity surfaces create a low temperature gradient region and eliminate the natural convection effects. As for conventional straight fin configuration, it produced thinner melt front with smaller radius of vortex circulations due to the high thermal resistance solid PCM at the melting interface.

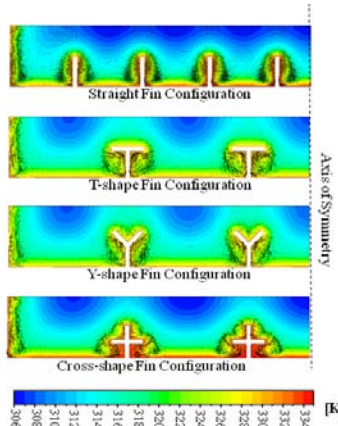


Figure 7 Temperature distribution and flow field visualization of straight fin, T-shape fin, Y-shape fin and cross-shape fin type at 2000s.

As heating continues, the melting patterns for all four configuration became abrupt as more liquid fractions were formed. Heat conduction became weaker and natural convective effect became dominant after 2000 seconds of melting. The temperature-driven buoyancy forces assisted PCM melting by dissipating heat to the surrounding cooler regions of the PCM along the solid-liquid interface. The benefit of the horizontally extended side fin extended (T-shape, Y-shape fin and cross-shape fin) dissipates heat more evenly within the rectangular encapsulation shown in the contour of temperature distributions visualization in figure 7. When the encapsulation is nearly melted, the natural convective flow fields at T-shape, Y-shape except for cross-shape fin were disrupted by the present of horizontal side fins. The buoyancy effect and gravity are normal to the heating base and the free circulating natural convective vortices are obstructed by the horizontal fins which affects the heat distribution internally. Hence, shorter horizontal fin may be more effective at this stage. Cross-shape fin has shown more natural convective vortices formed at the top surface of the fin by the assisted by the top vertical and horizontal fin surface. However, at the lower regions has an adverse natural convective performance where there is poor circulating vortices seen in figure 8. As for straight fin configuration, it developed steady melting front and vortices formation at aluminum surfaces at the 2000 seconds time. The natural convection heat transfer became better as the vortices were not restricted and able to grow rapidly in the later stage. This phenomenon also shows that the natural convection

current played a major role in reducing the thermal resistance of the PCM in the encapsulation.

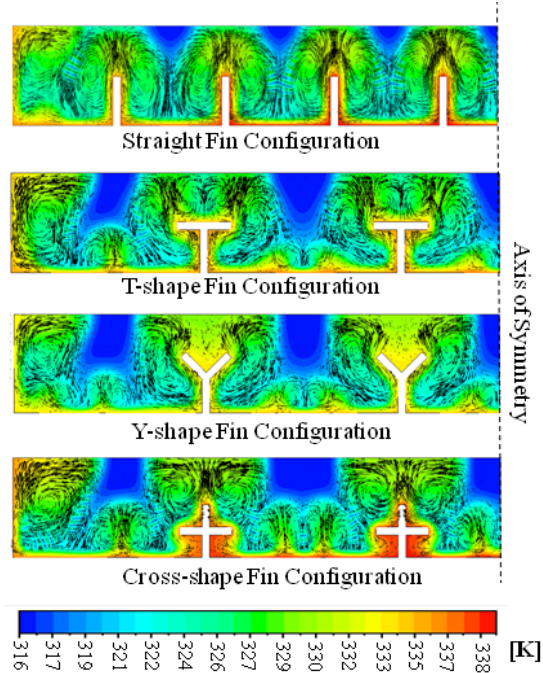


Figure 8 Temperature distribution and flow field visualization of rectangular fin, T-shape fin, Y-shape fin and cross-shape fin type at 4000s.

E. Effects on Fin Length and Geometrical Shapes

Figure 9 shows the melt fraction comparison between finless, eight straight fins installation, four long straight fins installation and four cross-shape fins installation in the same rectangular encapsulation with similar volume of PCM. Due to similar temperature distribution as straight fin melting, the above cross-shape fin configuration was selected for comparison. It is very interesting to see that finless configuration has faster liquid PCM formation at the earlier stage but melting rate maintains steady over time.

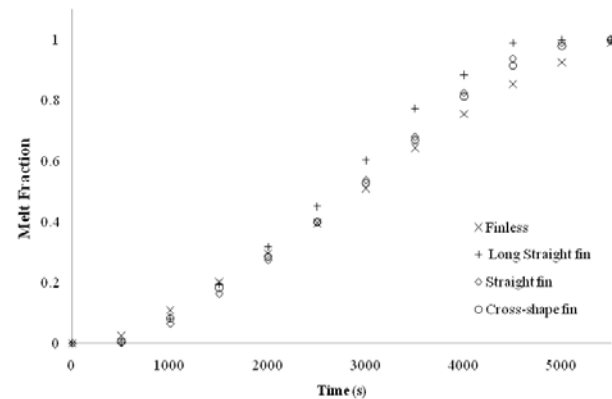


Figure 9: Melt fraction comparison for different fin configurations

During initial stage, only conduction heat transfer is present in all PCM melting at the solid stage regardless of organic or

inorganic PCM category. Because of the high thermal resistance within the solid PCM ($\sim 0.2\text{W/m K}$, paraffin wax), the heating base will generate high temperature region which reaches its melting point at earlier stage causing early liquid formation at the base. At the latter stage, the natural convective effect has maintained the melting rate as the thermal conductivity of liquid PCM ($\sim 0.15\text{W/m K}$) is lower than solid PCM. The 2-long fins configuration has the best melting performance in this comparative study despite having slower melt fraction formation at the initial stage. The effective thermal conductivity is higher as compared to finless configuration due to the present of high thermal conductive aluminum fin ($\sim 200\text{W/m K}$), resulting a lower temperature gradient at the heating base.

IV. CONCLUSIONS AND FUTURE WORKS

In this numerical investigation, four T-shape fins, Y-shape fins and cross-shape fins configurations have been compared with the conventional eight straight fins configuration. The comparative melt fraction results have revealed that fin shape alteration do has certain effect on melting performance. These investigated fin shapes are able to deliver comparable melting rate as higher number of conventional straight fins installed in the same rectangular encapsulation. The present of horizontal aluminum side fins which extended into the core of the PCM have influenced heat conduction and natural convection heat transfer within the PCM encapsulation. This approach allows PCM thermal storage designers to have another option of using lesser fins for similar melting performance by changing the geometrical shape of the fins. As the horizontally extended side fins affect the vortices formation driven by temperature gradient, further researches are needed to investigate on the optimum fin gap and shape for promoting higher melting rate through optimizing both conduction and natural convective effects during phase change.

ACKNOWLEDGMENT

The authors wish to thank Dr. Panniselvam from Department of Chemical Engineering RMIT University for his kind support in providing thermo-physical properties of the paraffin wax.

REFERENCES

- [1] Morisson, Abdel-Kalik, "Effect of phase change energy storage on the performance of air-based and liquid-based solar heating system," *Solar Energy* 20 (1978) 57-67.
- [2] A.A. Ghoneim, "Comparison of theoretical models of phase-change and sensible heat storage for air and water-based solar heating systems. *Solar Energy* 42 (1989) 209-220.
- [3] A.G. Evans, M.Y. He, J.W. Hutchinson, "Temperature distribution in advanced power electronics systems and the effect of phase change materials on temperature suppression during power pulses," *J. Electron. Package.-Trans. ASME* 123 (2001) 211-217.
- [4] S. Jegadheeswaram, S.D. Pohekar, "Performance enhancement in latent heat thermal storage system: A review," *Renewable and Sustainable Energy Reviews* 13 (2009) 2225-2244.
- [5] S.M. Hasnain, "Review on sustainable thermal storage technologies, Part 1: Heat storage materials and techniques," *Energy Convers Mgmt* 39 (1998) 1127-1138.
- [6] M. Gharebagi, I. Sezai, "Enhancement of heat transfer in latent heat storage modules with internal fins," *Numer Heat Transf Part A* 53 (1997) 749-765.
- [7] M. Lacroix, M. Benmadda, "Numerical simulation of natural convection-dominated melting and solidification from a finned vertical wall," *Numer. Heat Transfer Part A-Appl.* 31 (1997) 71-86.
- [8] P. Lamberg, K. Siren, "Numerical and experimental investigation of melting and freezing processes in phase change material storage," *Int J. Therm Sci* 43(2004) 277-287.
- [9] W.R. Humphries, E.I. Griggs, "A design handbook for phase change thermal control and energy storage devices," *NASA Technical Paper 1074*, NASA Scientific and Technical Information Office, 1977.
- [10] R. Reid, J. Prausnitz, B. Poling, "The Properties of Gases and Liquids," McGraw-Hill, New York, 1987.
- [11] V. Shatikan, G. Ziskind, R. Letan, "Numerical investigation of a PCM-based heat sink with internal fins," *Int. J. Heat and Mass Transfer* 48 (2005) 3689-3706.
- [12] A.D. Brent, V.R. Voller, K.J. Reid, "Enthalpy-porosity technique for modeling convection-diffusion phase change: Application to the melting of a pure metal," *Numer. Heat Transfer* 13 (1988) 297-318.